Kinetics and Thermal Properties of Epoxy Resin Cured with Ni(II)-tris-(*O*-pheneylendiamine) bromide

Abdollah Omrani,[1,2] Abbas Ali Rostami,[1] Mousa Ghaemy[1]

[1]*Department of Chemistry, University of Mazandaran, Babolsar, Mazandaran, Iran*
[2]*Department of Mechanical and Material Engineering, University of Western Ontario, Ontario N6A 5B9, Canada*

Received 14 March 2005; accepted 7 September 2005
DOI 10.1002/app.23180
Published online 14 April 2006 in Wiley InterScience (www.interscience.wiley.com).

ABSTRACT: Diglycidyl ether of bisphenol A (DGEBA) is cured with a nickel complex of *O*-phenylendiamine (OPD) as a ligand. The structure of the synthesized curing agent is confirmed through IR and elemental analysis. The curing kinetics of DGEBA/$Ni(OPD)_3Br_2$ system is studied by the dynamic DSC and isothermal FTIR techniques. In all cases, we have observed at least two exothermic peaks during DSC traces up to 350°C. Dynamic activation energies are calculated by using the two isoconversional, Kissinger and Ozawa, methods applied to peak maximum. A two-parameter (*m*, *n*) autocatalytic model (Sestak–Berggren equation) is found to be the most adequate model to describe the cure kinetics of the observed thermal events. Isothermal kinetic parameters are estimated using the Horie model. The onset decomposition temperature and char yield (at 700°C) of the crosslinked material were 290°C and 27%, respectively. The activation energy of the solid-state thermal degradation process is evaluated by Ozawa approach, resulting in 95–138 kJ/mol on a range of 2–20% decomposition conversion.
 J Appl Polym Sci 101: 1257–1265, 2006

Key words: activation energy; calorimetry; metal-organic catalysts; thermosets

INTRODUCTION

Epoxy resins are the most important class of thermosetting resins and find application in surface coating, composite matrices, adhesive, encapsulation of electronic components, and aerospace industries.[1] The physical, mechanical, and electrical properties of thermosetting polymers depend to a large extent on the degree of cure. On the other hand, the processability of a thermoset resin critically depends on the rate and extent of polymerization under process conditions. Therefore, kinetic characterization of the epoxy resin is not only important for a better understanding of structure–property relationships, but also fundamental in optimizing process conditions and product quality. The curing of thermosets and, particularly, the cure of epoxy resin involves the formation of a rigid three-dimensional network by the reaction with hardeners that have more than two reactive functional groups. The chemistry of cure is initiated by the formation and linear growth of the chain, which soon begins to branch and then to crosslink. As the cure proceeds, the molecular weight increases rapidly. The size of the molecule increases and several chains become linked together into networks of infinite molecular weight.

This transformation from a viscous liquid to an elastic gel is sudden and irreversible and marks the first appearance of the infinite network. The curing process can be started with a wide range of curing agents such as amines, amides, anhydrides, isocyanates, and aminoformaldehyde resins.[2,3] Excellent reviews of the mechanism and kinetics of thermosetting materials have appeared in the literature.[4,5] A number of experimental techniques and studies related to the thermosetting cure reactions have been reported in the literature, with emphasis on the chemical, physical, and mechanical property changes with time.[6,7] Cure kinetics models are generally developed by analyzing experimental results obtained by differential scanning calorimetry (DSC).[8–11]

Kurnoskin[12–16] has reported the hardening, structure, and properties of epoxy oligomers with the chelates of the general formula $[M(R)_n(X)_p]$. Recently, the development of controllable curing agents based on metal chelates for epoxy resins have been addressed by Hamerton and coworkers.[17–19] Generally, metal-organic curing agents have some advantages regarding long pot life, physical properties, thermal stability, chemical resistance, and electrical characteristics. In the present work, we investigated the cure kinetic of DGEBA with an inorganic complex of Ni(II) with *O*-pheneylendiamine (OPD) as a ligand under both dynamic and isothermal conditions. Some properties of

Correspondence to: A. Omrani (omrani@umz.ac.ir and aomrani@uwo.ca).

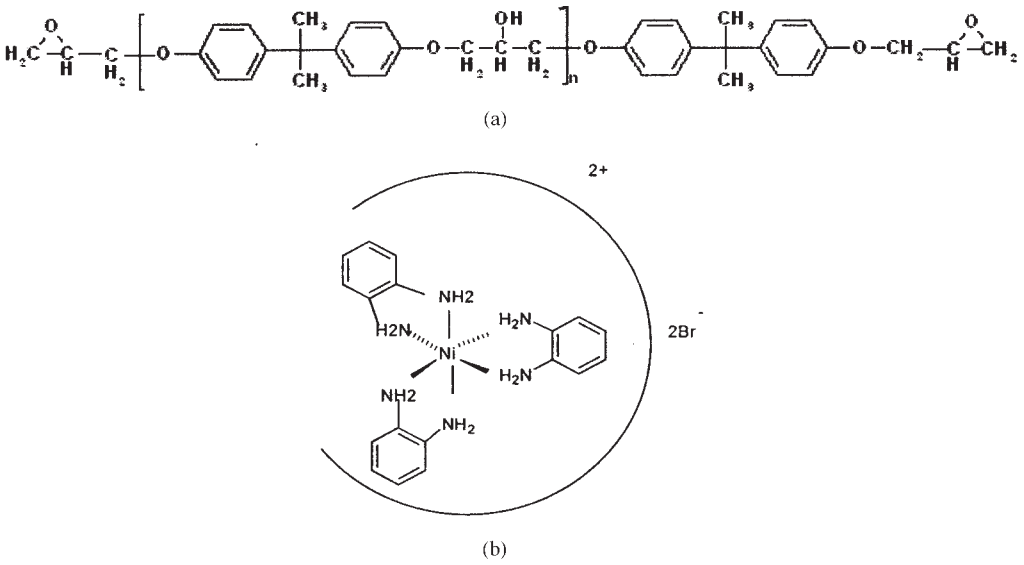

Figure 1 Structures of chemicals used: (A) DGEBA and (B) $Ni(OPD)_3Br_2$.

$Ni(OPD)_3X_2$ (X = Cl and Br)-epoxy blends, such as dissociation, thermal, and storage behaviors, have been studied by Hamerton et al.[17] However, cure kinetics of DGEBA/$Ni(OPD)_3Br_2$ system is not reported in the literature in detail. Figure 1 shows the structure of epoxy resin and curing agent.

EXPERIMENTAL

Materials

O-phenylendiamine (OPD) and nickel bromide three hydrate were used from the Fluka Chemical Company. OPD was purified using a standard method. All solvents used in the present work were always degassed with high pure nitrogen prior to use. The epoxy resin was Epon 828 from Shell Chemical Company, with an epoxy equivalent weight of about 185 equiv/g determined by wet analysis method.[20]

Characterization

DSC measurements are carried out with a Du Pont DSC 910 system supported with a pc computer for data acquisition. The DSC is calibrated with high-purity indium before any experiment. Dynamic data are obtained with about 3 mg samples in a nitrogen atmosphere (40 cm^3/min) at a heating rate of 5–20°C/min. Isothermal cure reaction data are monitored at four isothermal temperatures of 180, 190, 200, and 210°C, using a NICOLET 550 Magna FTIR system well-equipped with computer and OMINIC software for data analysis. Thermogravimetric analysis is done with a TA instrument TGA 1000M^+ at various heating rates of 5, 10, 15, and 20°C/min in air from room temperature to 900°C.

Synthesis of curing agent

The curing agent has been synthesized using the method reported by Hamerton et al.[17] Elemental analysis (C and H) of curing agent was determined by a LECO CHN-600. The content of nickel in the curing agent was also measured by BYJE ICP-plasma JY 138 instrument. Table I lists the elemental analysis results

TABLE I
Elemental Analysis of $Ni(OPD)_3Br_2$

Complex	% C	% H	% Ni
$Ni(OPD)_3Br_2$	39.7 (39.7)	4.35 (4.42)	10.9 (10.81)

The requested values are given in parenthesis.

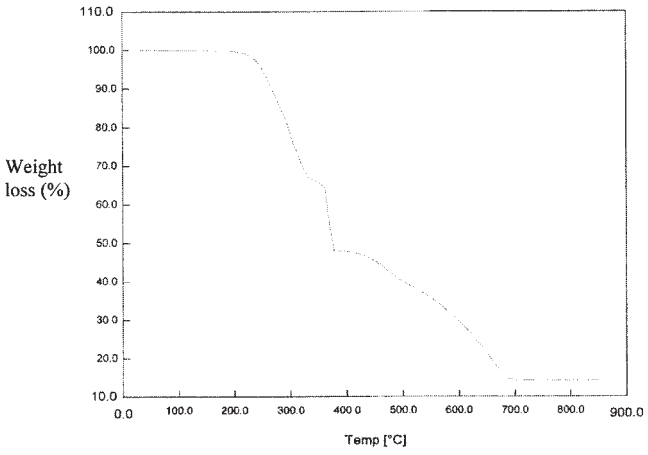

Figure 2 TG thermogram of the curing agent.

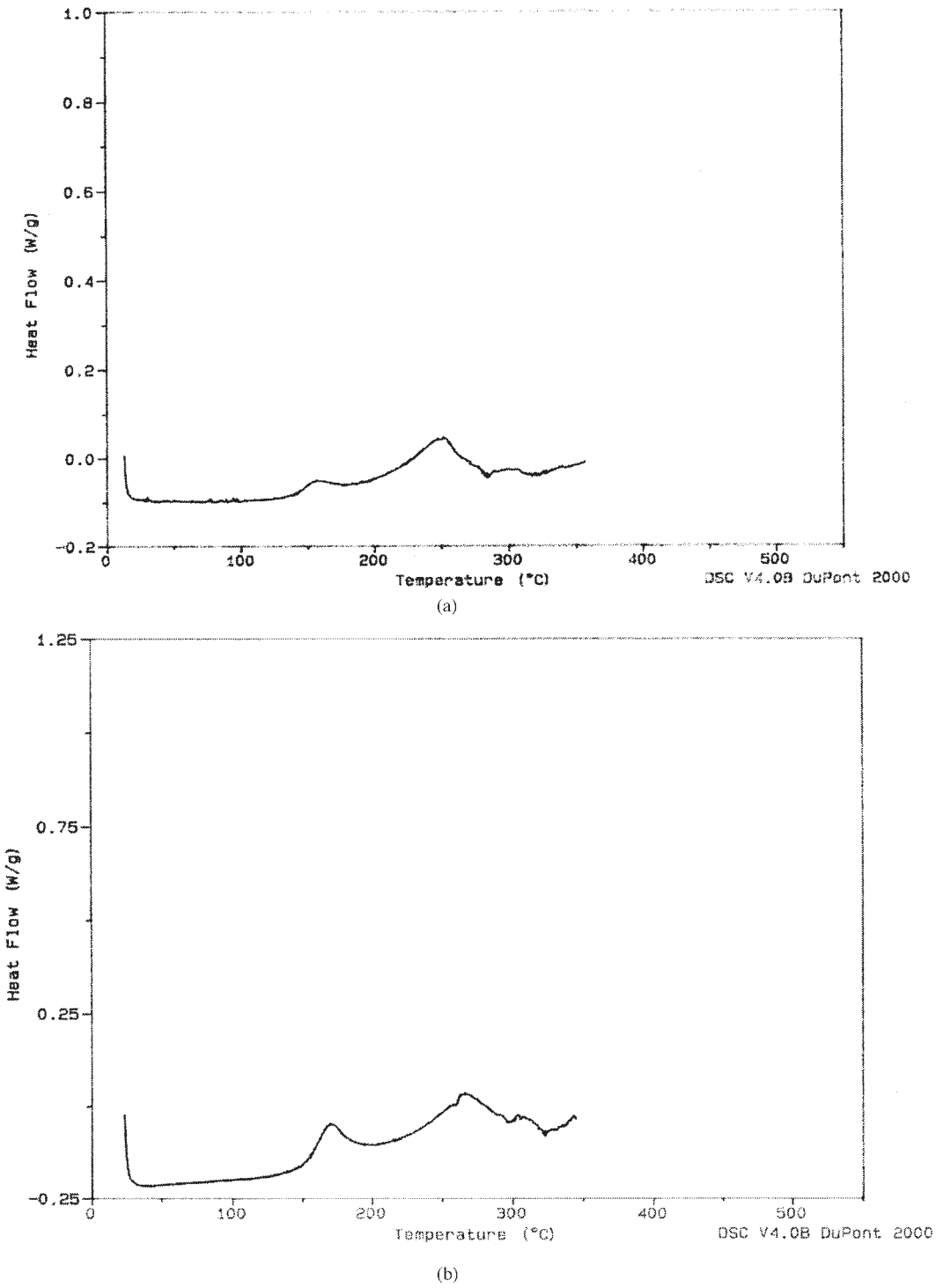

Figure 3 DSC heating scans of epoxy cured with $Ni(OPD)_3Br_2$ at (a) 5 and (b) 10°C/min.

of the curing agent, and these are compared with the required values.

Thermogravimetry analysis of $Ni(OPD)_3Br_2$

Figure 2 shows the TGA curve of $Ni(OPD)_3Br_2$ in nitrogen atmosphere (flow 30 cm^3/min) at heating rate of 20°C/min. As can be seen, there is a multi-step and complex thermal dissociation behavior for the system as verified by the results obtained by Hamerton et al.[17] Obviously, the delivery of the ligand (OPD) is a gradual process and occurs on a broad range of temperature about 220–400°C (prior to the final dissociation step). Two significant thermal events are

TABLE II
Curing Characteristics of the Two Exotherms as Obtained from DSC Curve Analysis

Complex	Heating rate (°C/min)	Cure onset[a] (°C)	1st peak max (°C)	2nd peak max (°C)	ΔH_{Total}[b] (J/g)
$Ni(OPD)_3Br_2$	5	125	156.17	251.77	54.294
	10	138.6	169.86	266.5	49.17
	15	150.7	176.85	278.33	40.431
	20	157	186.78	294.24	58.224

[a] Cure onset temperature is considered as onset of the first exotherm.
[b] The total enthalpy is the sum of enthalpy changes for the both exotherms.

observed; the first one occurred at 220°C with about 32% loss in mass and the second one appeared at 350°C with about 16% loss in mass, followed by final breakdown of the curing agent between 420 and 650°C. This gradual removal of the ligand in the nickel complex could be responsible for the two expanded exothermic peaks observed during DSC traces. However, TGA curve is taken in isolation form, and thermal dissociation pattern in epoxy matrix is a more complex process.

Formulation of epoxy-nickel complex compositions

From the comparison point of view, the level of curing agent incorporated into epoxy was 10 phr for all measurements reported in the present study, i.e., DSC and FTIR experiments. The curing agent must be dried in vacuo and powdered completely prior to preparation of the epoxy compositions. Then, the mixture is stirred manually for about 15 min until the curing agent is satisfactorily dissolved in the epoxy. To facilitate mixing, a small volume of acetone is added to the epoxy compositions. From the above mixture, samples of about 3 mg are utilized in DSC experiments. Isothermal curing traces are carried out on a very thin film of the freshly prepared epoxy mixtures between two KBr disks. FTIR spectra are monitored at various times during the cure process.

RESULTS AND DISCUSSION

Figure 3(a,b) shows representative DSC curves of epoxy resin cured with $Ni(OPD)_3Br_2$ at two different heating rates. As seen from the DSC curves, higher curing onset temperature is a characteristic of the system. In all cases, we have recorded two distinct exotherms during DSC traces up to 350°C. A third exothermic peak has been seen at higher temperatures and was not considered for further investigation due to significant contribution of thermal degradation process ongoing at higher temperatures. Table II lists some characteristics of the two exotherms.

Cure kinetics of DGEBA/$Ni(OPD)_3Br_2$ system under dynamic conditions

The activation energies of the curing reaction can be estimated by dynamic or isothermal experiments. For dynamic DSC scans, activation energy was calculated from the plots of heating rate versus reciprocal of

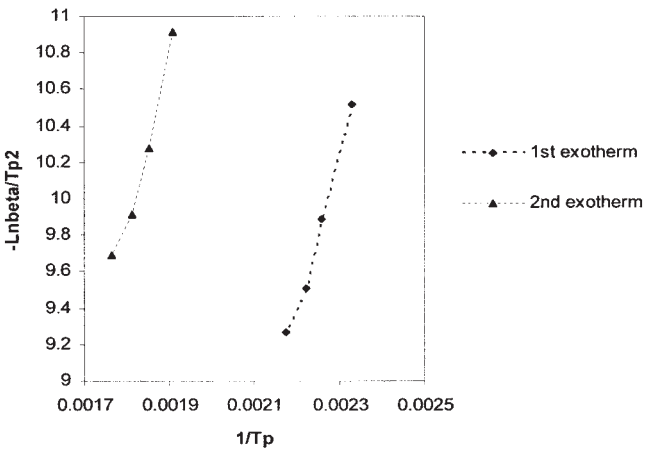

Figure 4 Kissinger method is applied to DSC exotherms.

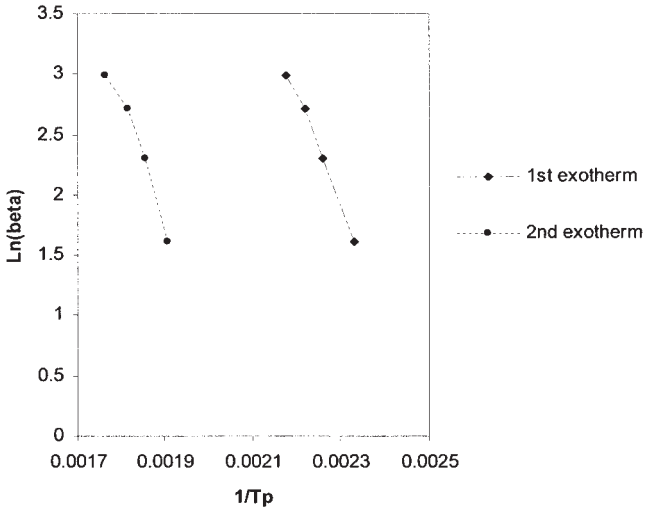

Figure 5 Ozawa method is applied to DSC exotherms.

TABLE III
Activation Energies are Calculated using the Kissinger and Ozawa Methods and their Average Values

Complex	Exotherm	E_a (kJ/mol) Kissinger	Ozawa	Average
$Ni(OPD)_3Br_2$	First	68.6237	72.221	70.4223
$Ni(OPD)_3Br_2$	Second	71.8704	76.939	74.4047

exotherm peak temperature, by means of the two isoconversional, Kissinger[21] and Ozawa-Flynn-Wall,[22] methods.

Dynamic method I (Kissinger method)

The data from dynamic DSC measurements are analyzed with the following equation:

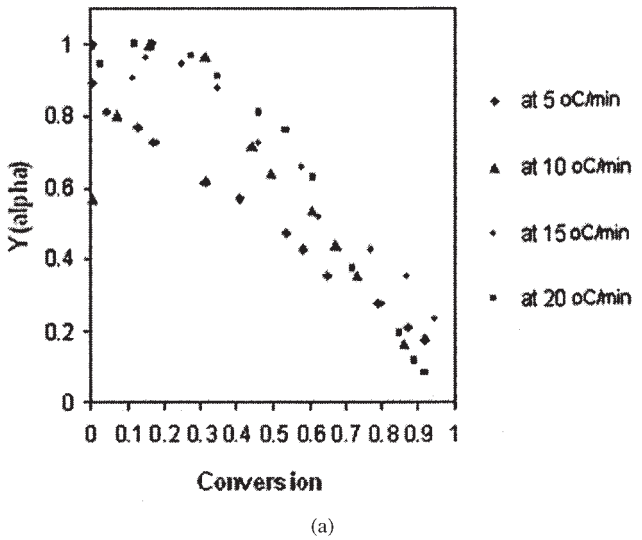

(a)

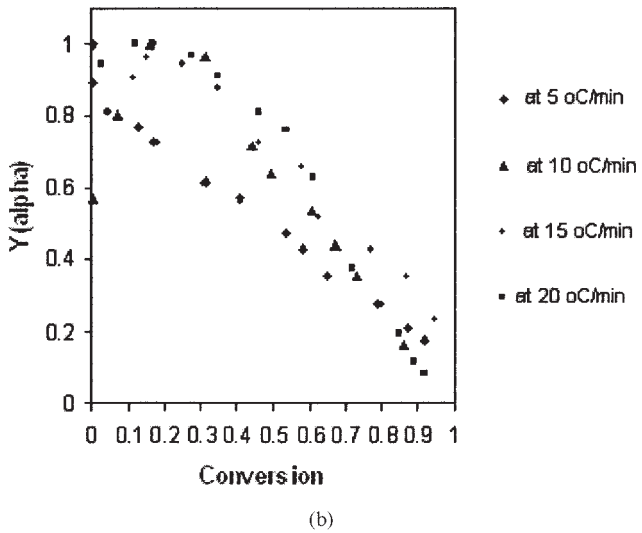

(b)

Figure 6 Variation of $Y(\alpha)$ function for the first exotherm (a) and the second exotherm (b).

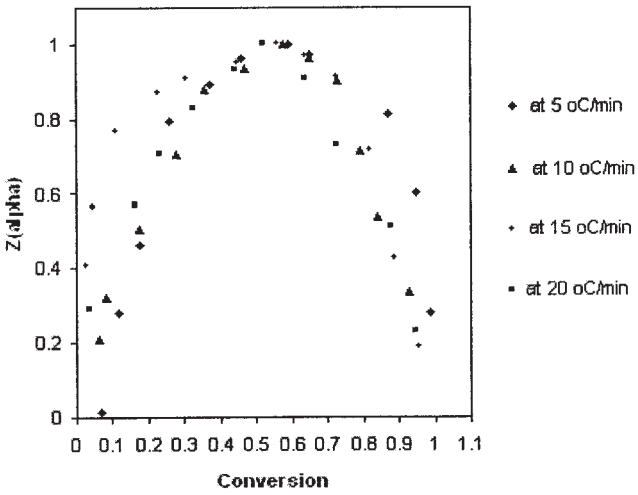

(a)

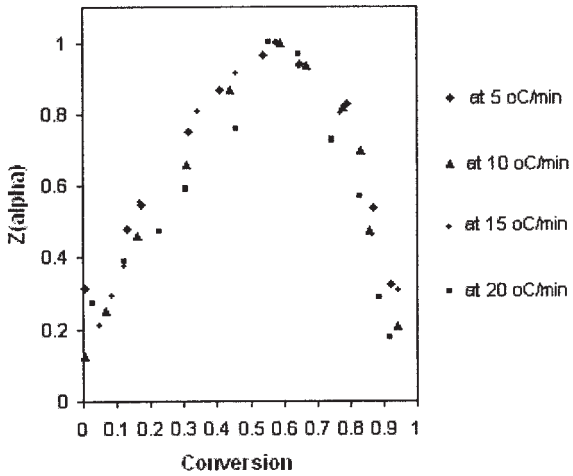

(b)

Figure 7 Variation of $Z(\alpha)$ function for the first exotherm (a) and the second exotherm (b).

$$-\ln(\beta/T_p2) = E_a/RT_p + \ln(E_a/R) - \ln(An) - (n-1)\ln(1-\alpha)_p \quad (1)$$

A plot of $-\ln(\beta/Tp2)$ against $1/Tp$ gives a straight line. The activation energy is estimated using the corresponding plots. Figure 4 displays Kissinger plots of both exotherms.

Dynamic method II (Ozawa method)

The activation energy can be calculated using Ozawa method based on the following equation:

$$\log\beta = (1/2.303)\ln\beta = -0.4567E_a/RT + (\log(AE_a/R) - \log(f(\alpha)) - 2.315) \quad (2)$$

TABLE IV
The Values of α_p, α_M, and $\alpha_p\infty$ Obtained from the DSC Curve Analysis

Exotherm	Heating rate (°C/min)	α_p	α_M	$\alpha_p\infty$
First	5	0.51	0.26	0.59
	10	0.48	0.215	0.577
	15	0.49	0.181	0.56
	20	0.52	0.164	0.523
Second	5	0.58	0.0063	0.58
	10	0.497	0.16	0.593
	15	0.52	0.174	0.58
	20	0.59	0.125	0.562

where, $f(\alpha)$ is the conversion dependence term. Thus, at the same conversion, a plot of ln β versus $1/T_p$ gives a liner plot with a slope of 1.052 E_a/R. The corresponding plots for the two exotherms are shown in Figure 5. Table III presents the activation energies and the average values of the two exothermic peaks.

Evaluation of kinetic parameters of the two thermal events

The average values of activation energies obtained by the two isoconversional methods are used to find the appropriate kinetic models that best describes the cure reaction. For this purpose, we need to appeal to the specific functions of $Y(\alpha)$ and $Z(\alpha)$.[23,24]

$$Y(\alpha) = (d\alpha/dt)ex \quad (3)$$

$$Z(\alpha) = \pi(x)(d\alpha/dt)T/\beta \quad (4)$$

where, x is the reduced activation energy (E_a/RT), β is the heating rate (K/min), T is the absolute temperature (K), and $\pi(x)$ is the expression of the temperature integral, which can be well-expressed as follows[25]:

$$\Pi(x) = (x3 + 18 \times 2 + 88x + 96)/ \times (x4 + 20 \times 3 + 120 \times 2 + 240x + 120) \quad (5)$$

The $Y(\alpha)$ function is proportional to $f(\alpha)$ function, being characteristic for a given model. Both $Y(\alpha)$ and $Z(\alpha)$ functions are normalized within the (0,1) interval. The characteristics of both $Y(\alpha)$ and $Z(\alpha)$ functions permit us to find the most adequate kinetic model to describe each exotherm. It is also possible to estimate the pre-exponential factor, A, after finding the kinetic model by means eq. (6):

$$A = -(\beta x_p)/(Tf'(\alpha_{p)) \exp(} x_p) \quad (6)$$

where, $f'(\alpha_p)$ is the differential form of the kinetic model. The calculated $Y(\alpha)$ and $Z(\alpha)$ functions for the two exotherms are shown in Figure 6(a,b) and Figure 7(a,b), respectively. These functions give a maximum value at α_M (for $Y(\alpha)$) and $\alpha_p\infty$ (for $Z(\alpha)$), which are used to decide the choice of the kinetic model. Table IV lists the values of maximum α_M and $\alpha_p\infty$ together with α_p of the exotherms. It can be concluded from the data in Table IV that for both exotherms of the studied system, the values of α_M are lower than α_p, while $\alpha_p\infty$ exhibits values lower than 0.632.

These remarks indicate that the two observed curing peaks can be described by the two-parameter Sestak–Berggren autocatalytic model.[26] The SB (m, n) kinetic model can be described as $f(\alpha) = \alpha^m(1 - \alpha)^n$, where m and n are the kinetic exponents. The kinetic parameter n is calculated by the slope of the linear plots of $\ln[(d\alpha/dt)e^x]$ against $\ln[\alpha^p(1 - \alpha)]$. The values of m are also estimated using the equation $m = p \times n$, where $p = \alpha_M/(1 - \alpha_M)$. Table V lists the calculated kinetic parameters with the SB (m, n) kinetic model.

Cure kinetics of DGEBA/Ni(OPD)$_3$Br$_2$ system under isothermal conditions

The curing reaction of epoxy resin with nickel complex is studied at four isothermal temperatures of 180,

TABLE V
The Kinetic Parameters Evaluated using the SB (m, n) Model

Exotherm	Heating rate (°C/min)	n	Mean	m	Mean	ln A	Mean
First	5	0.481		0.169		15.229	
	10	0.623	0.406	0.171	0.112	15.409	15.335
	15	0.292		0.064		15.398	
	20	0.227		0.0445		15.302	
Second	5	0.685		0.0043		11.889	
	10	1.474	0.961	0.281	0.143	12.148	11.922
	15	0.644		0.136		11.908	
	20	1.042		0.149		11.743	

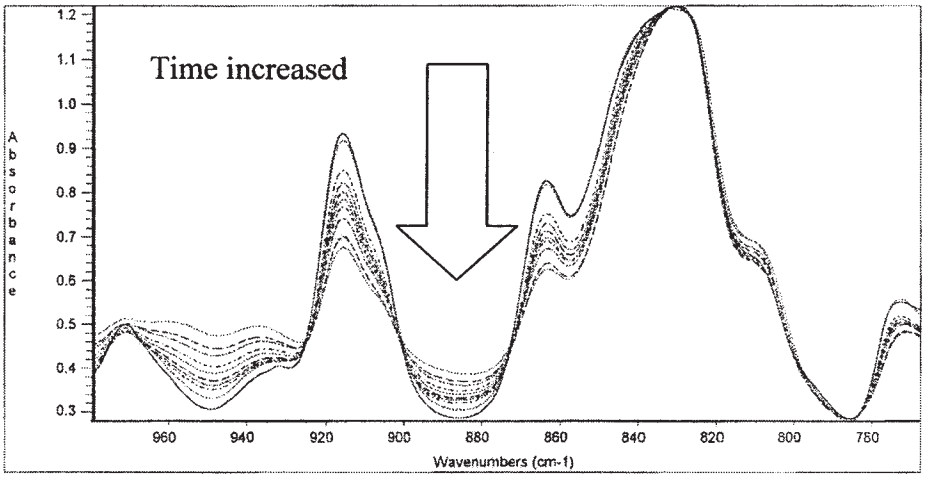

Figure 8 Representative FTIR spectra of epoxy cured with $Ni(OPD)_3Br_2$ at 180°C at different cure times.

190, 200, and 210°C, using FTIR technique. FTIR spectra are monitored along with the progress of the cure reaction and analyzed by the TA commercial software. The conversion of epoxy groups is calculated using the ratio of normalized epoxide peak at a specific time, t, to normalized epoxide peak at $t = 0$. Representative FTIR spectra at 180°C are shown in Figure 8. The reaction rate and conversion plots are also depicted in Figures 9 and 10, respectively. It is seen that the reaction rate is affected by the isothermal temperature and the reaction time. The higher is the isothermal temperature, the shorter the reaction times to complete the curing reaction. To determine the kinetic parameters, we utilized the kinetic model proposed by Horie et al.[27] to isothermal data. A general form of the reaction rate for this model is as follows:

$$d\alpha/dt = (K_1 + K_2\alpha)(1 - \alpha)^n \qquad (7)$$

The different amounts of n selected usually makes it possible to obtain a good fitting of experimental data. The reaction order is determined using the model, and the reduced rate of reaction is defined as follows:

$$\alpha^0 = (d\alpha/dt)/(1 - \alpha)^n = K_1 + K_2\alpha \qquad (8)$$

Different values of n (0.5, 1, 1.5, and 2) are checked to obtain the best fitting of the experimental results. Plots of reduced rate, α^0, versus conversion for different values of n at 180°C are shown in Figure 11. The best linear fitting of the experimental results is attained for $n = 2$ at all isothermal temperatures. Once this value is found, it may be concluded that the overall reaction order is 3. Table VI exhibits the rate constants corre-

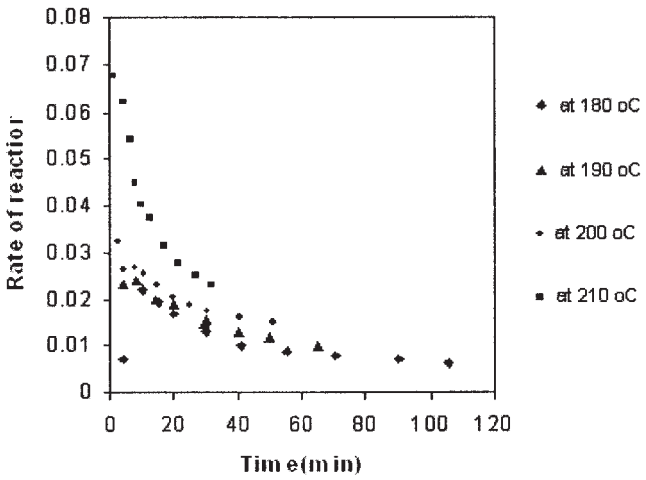

Figure 9 Reaction rate versus time plots at different isothermal temperatures.

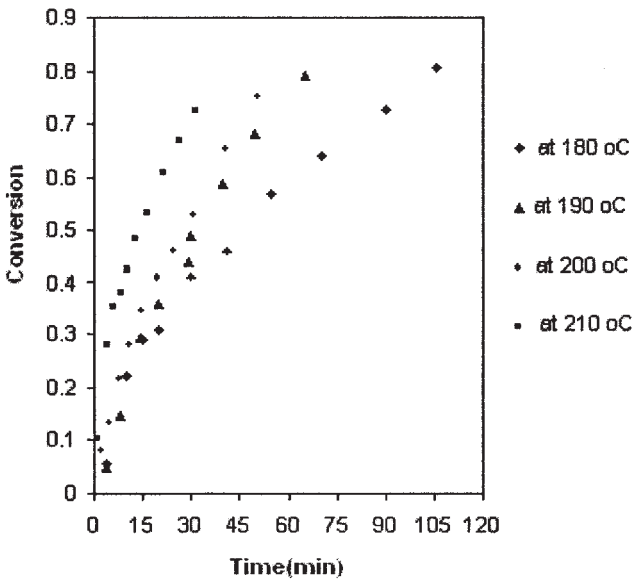

Figure 10 Degree of conversion against time curves at various isothermal temperatures.

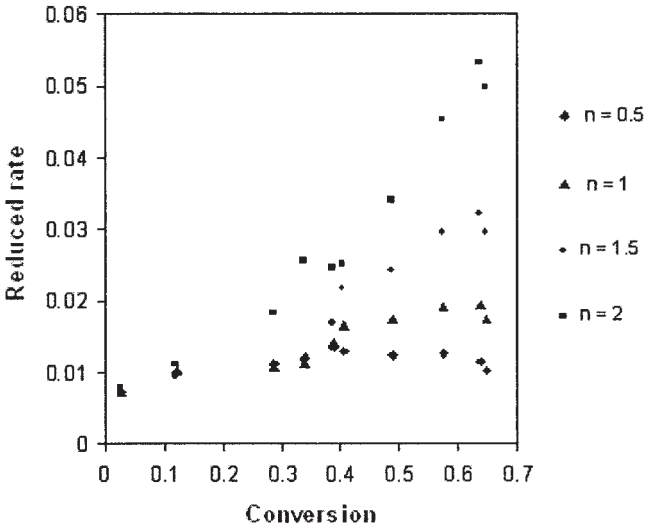

Figure 11 Plots of reduced rate against conversion for different n values at 180°C.

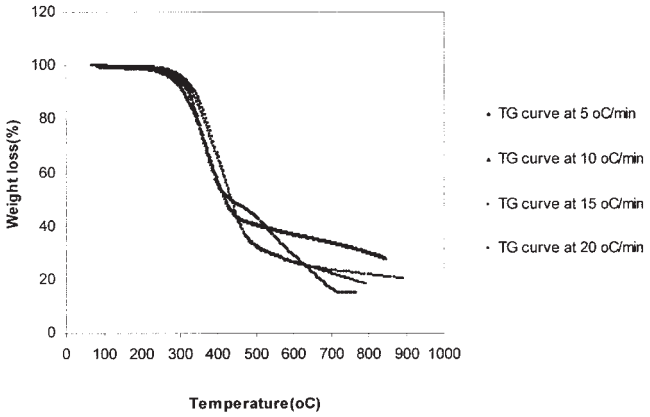

Figure 12 TG curves of DGEBA/Ni(OPD)$_3$Br$_2$ system at various heating rates in air.

sponding to the nth order and autocatalytic mechanisms at various isothermal temperatures. The activation energies corresponding to the two kinetic mechanisms are obtained from the Arrhenius plots of ln K against $1000/T$ and are too listed in Table VI. As it can be seen from the results in Table VI, there is a good agreement between the total value of activation energy obtained by Kissinger method (140.4941 kJ/mol) and the sum of the nth order and the autocatalytic paths activation energies determined from isothermal experiments (136.17 kJ/mol).

Thermal properties of cured epoxy

TGA traces of the epoxy resin containing nickel complex provided additional information considering their thermal stability and thermal degradation kinetics. For the TG measurements, an epoxy-Ni(OPD)$_3$Br$_2$ (10 Phr) mixture has been cured isothermally at 200°C for 5 h. The completeness of curing is confirmed by the disappearance of the epoxy characteristic absorption band at 916 cm^{-1} in the IR spectrum.

The samples of about 5 mg are separated and it undergoes TG analysis from room temperature to 900°C in air. TGA curves of the sample at various heating rates are shown in Figure 12. TGA trace of the cured epoxy at 5°C/min revealed two decomposition steps. This may be described by an oxidative degradation mechanism of carbonaceous residue, which is more possible at slow heating scans. The onset temperature of the degradation and the char yield (at 700°C) are found to be 290°C and 27%, respectively, at the heating rate of 20°C/min. This high char yield exhibits that the flame retardancy property of the produced thermosetting materials is considerable.

Activation energy of thermal degradation

The activation energy is determined by the Ozawa method. Because of the complex thermal degradation behavior of the system at low heating rate, i.e. 5°C/min, the activation energy has been calculated only before decomposition conversion less than 21%. The ln β versus $1000/T$ plots of the system at different decomposition conversions are constructed, and the degradation activation energies at different conversion are determined and shown in Figure 13.

CONCLUSIONS

A nickel-containing epoxy polymer is produced through the curing of a bisphenol A type epoxy with a nickel complex of *O*-phenylendiamine. The reaction

TABLE VI
Values of Rate Constants and Activation Energies Calculated with the Horie Model

Temperature (°C)	K_1 (nth order)	K_2 (Autocatalytic)	E_a (kJ/mol)	
			nth order	Autocatalytic
180	0.0004	0.0739		
190	0.0073	0.1101	54.4	81.8
200	0.0096	0.1455		
210	0.0131	0.3028		

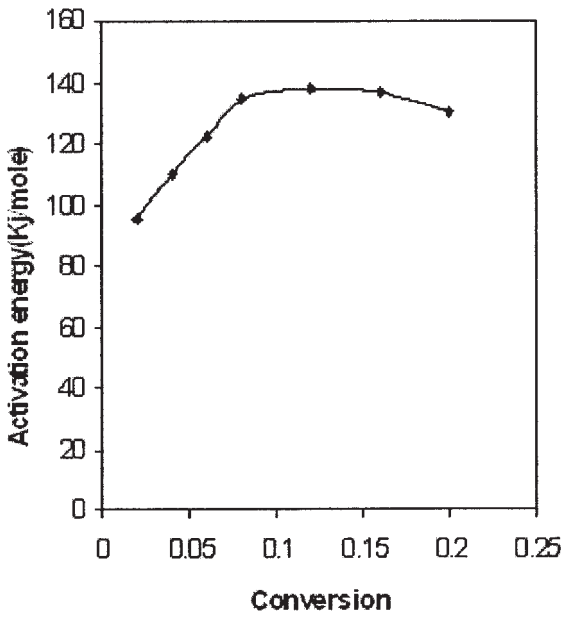

Figure 13 The thermal degradation activation energies at different conversions.

kinetics of $Ni(OPD)_3Br_2$-cured epoxy resin is studied by both the dynamic DSC and the isothermal FTIR techniques. Two generalized kinetic, Kissinger and Ozawa, methods are employed to determine the activation energies. DSC curves showed two distinctly separated exothermic peaks at all heating rates. The total value of activation energy obtained using the two methods are in reasonable concordance, demonstrating the capability of FTIR-based kinetic analysis in the modeling of curing behavior of epoxy-metalorganic curing agent systems. It is established that the two-parameter autocatalytic model (Sestak–Berggren equation) is a suitable model to elucidate of kinetic behavior of the studied epoxy system. It is also shown that thermal stability and weight loss rates of epoxy resin improved by incorporating nickel complex into epoxy matrix.

A. Omrani gratefully acknowledges Dr. K. Nouri for the TGA facility in Western campus and for the valuable discussions.

References

1. Feldman, D.; Barbalata, A. Synthetic Polymers: Technology, Properties and Applications; Chapman & Hall: London, 1996; Chapter 8, p 316.
2. Ashcroft, W. R. In Chemistry and Technology of Epoxy Resin; Ellis, B., Ed.; Chapman & Hall: London, 1993; Chapter 2, p 21.
3. Buckhall, C. B. Toughened Plastics; Wiley: New York, 1997.
4. Barton, J. M. Adv Polym Sci 1985, 72, 111.
5. Rosenberg, B. A. Adv Polym Sci 1986, 75, 113.
6. Warfield, R. W.; Petric, M. C. J Polym Sci 1959, 37, 305.
7. Lewis, A. F.; Gillham, J. K. J Appl Polym Sci 1962, 6, 422.
8. Guthner, T.; Hammer, B. J Appl Polym Sci 1993, 50, 1453.
9. Su, C. C.; Woo, T. M. Polymer 1995, 36, 2883.
10. Khanna, U.; Chanda, M. J Appl Polym Sci 1993, 49, 319.
11. Lin, S. T.; Huang, S. K. J Appl Polym Sci 1996, 62, 1641.
12. Kurnoskin, A. V. Polymer 1993, 34, 1060.
13. Kurnoskin, A. V. Polymer 1993, 34, 1068.
14. Kurnoskin, A. V. Polymer 1993, 34, 1077.
15. Kurnoskin, A. V. Ind Eng Chem Res 1992, 31, 524.
16. Kurnoskin, A. V. Polym Compos 1993, 14, 481.
17. Hamerton, I.; Hay, J. N.; Howlin, B. J.; Jepson, P.; Mortimer, S. J Appl Polym Sci 2001, 80, 1489.
18. Brown, J.; Hamerton, I.; Hay, J. N.; Howlin, B. J. J Appl Polym Sci 2000, 15, 201.
19. Hamerton, I.; Hay, J. N.; Herman, H.; Howlin, B. J.; Jepson, P.; Gillies, D. G. J Appl Polym Sci 2002, 84, 2411.
20. Lee, H.; Neville, K. Handbook of Epoxy Resin; McGraw-Hill: New York, 1967.
21. Kissinger, H. E. Anal Chem 1957, 29, 1702.
22. Ozawa, T. Bull Chem Soc Jpn 1965, 38, 1881.
23. Malek, J. Thermochim Acta 1992, 200, 257.
24. Rosu, D.; Cascaval, C. N.; Mustata, F.; Ciobanu, C. Thermochim Acta 2002, 383, 119.
25. Monteserrat, S.; Malek, J. Thermochim Acta 1993, 228, 47.
26. Sestak, J.; Berggren, G. Thermochim Acta 1971, 3, 1.
27. Horie, K.; Hiura, H.; Sawada, M.; Mita, I.; Kamb, H. J Polym Sci 1970, 8, 1357.